catalysts

MDPI

Article

Ionic Liquid Modified SPION@Chitosan as a Novel and Reusable Superparamagnetic Catalyst for Green One-Pot Synthesis of Pyrido[2,3-*d*]pyrimidine-dione Derivatives in Water

Mohammad Hosein Sayahi [1,*], Asma Sepahdar [2], Farokh Bazrafkan [1], Farzaneh Dehghani [3], Mohammad Mahdavi [4] and Saeed Bahadorikhalili [5,*]

[1] Department of Chemistry, Payame Noor University (PNU), Tehran 19395-3697, Iran
[2] Department of Pharmaceutical Biomaterials, Faculty of Pharmacy, Tehran University of Medical Sciences, Tehran 14166-34793, Iran
[3] Department of Chemical and Petroleum Engineering, Sharif University of Technology, Tehran 11365-11155, Iran
[4] Endocrinology and Metabolism Research Center, Endocrinology and Metabolism Clinical Sciences Institute, Tehran University of Medical Sciences, Tehran 14166-34793, Iran
[5] Department of Electronic Engineering, Universitat Rovira i Virgili, 43007 Tarragona, Spain
* Correspondence: sayahymh@pnu.ac.ir (M.H.S.); saeed.bahadorikhalili@urv.cat (S.B.)

Abstract: In this paper, the chitosan-functionalized ionic liquid is modified with superparamagnetic iron oxide nanoparticles to form a novel and reusable catalyst (SPION@CS-IL), which was carried out using an ultrasonic promoted approach. Transmission electron microscopy (TEM), vibrating-sample magnetometer (VSM), energy-dispersive X-ray spectroscopy (EDX), Fourier transform infrared spectroscopy (FT-IR), X-ray powder diffraction (XRD), energy-dispersive X-ray spectroscopy (EDX), and thermogravimetric analysis (TGA) are some of the techniques that are used to fully characterize SPION@CS-IL. The created nanoparticles were discovered to be a reusable heterogeneous superparamagnetic catalyst for the environmentally friendly one-pot synthesis of pyrido[2,3-*d*]pyrimidine derivatives using a simple three-component reaction approach involving thiobarbituric acid, 4-hydroxy coumarin, and various aromatic aldehydes. The method is studied by performing the reaction under ultrasonic irradiation, while the approach is a "green" method, it uses water as the solvent. The isolated yields of the synthesized products are very advantageous. The catalyst has outstanding reusability and is easily removed from the products via filtration (5 runs). Short reaction times, low catalyst loadings, the nanocatalyst's capacity to be recycled five times, and the absence of harmful chemical reagents are all significant benefits of this environmentally benign process.

Keywords: SPION@CS-IL; superparamagnetic nanoparticle; green catalyst; Ultrasound irradiation; pyrido[2,3-*d*] pyrimidine-dione; multicomponent reaction

Citation: Sayahi, M.H.; Sepahdar, A.; Bazrafkan, F.; Dehghani, F.; Mahdavi, M.; Bahadorikhalili, S. Ionic Liquid Modified SPION@Chitosan as a Novel and Reusable Superparamagnetic Catalyst for Green One-Pot Synthesis of Pyrido[2,3-*d*]pyrimidine-dione Derivatives in Water. *Catalysts* **2023**, *13*, 290. https://doi.org/10.3390/catal13020290

Academic Editor: Elisabete Alegria

Received: 14 October 2022
Revised: 29 December 2022
Accepted: 18 January 2023
Published: 28 January 2023

1. Introduction

In modern synthetic chemistry, catalysis is important, whereas they are the cornerstones of green chemistry [1–5]. In chemistry labs and on industrial scales, catalysis is acknowledged as a crucial tool to develop a more sustainable chemical process. A suitable catalyst should have specified characteristics, such as cheap procurement costs, non-toxicity, outstanding activity, high stability, simple and efficient recovery, excellent recyclability, biocompatibility, and biodegradability, in accordance with the aforementioned reasons. Superparamagnetic iron oxide magnetic nanoparticles (MNPs) with biodegradable, biocompatible, superparamagnetic features that are non-cytotoxic to humans and other animals [6,7] have attracted great attention in various applications such as separation technology [8], protein immobilization [9], catalysis [10–16], medical science [17], and environment [18,19]. However, superparamagnetic iron oxide nanoparticles are unstable in physiological conditions and represent several disadvantages comprising easily oxidized in air, fast biodegradation, and loss of magnetism properties [20]. In addition, Superparamagnetic iron oxide magnetic nanoparticles (MNPs) are prone to aggregation because of their chemical activity, to overcome these obstacles, the modification of Superparamagnetic iron oxide MNPs has been carried out by several materials such as precious metals, carbon, silica, and biopolymers [21–27].

A remarkable biopolymer made from fishery wastes is chitin, which is an *N*-deacetylated chitosan derivative. It is a great material for creating new kinds of green catalytic systems because of its low cost, hydrophilicity, abundance, non-toxicity, biodegradability, and significant heat stability [28–31].

The fact that chitosan (CS) has free primary and secondary hydroxyl, as well as amine functional groups on its surface, is primarily responsible for the widespread use of the material as catalyst support. Catalysts based on chitosan have drawn a lot of interest because, in particular, the amine and hydroxyl groups provide active sites for a range of chemical changes [27,28,30,32–36].

Chitosan that has been functionalized with ionic liquid is one of the simple and appropriate ways to modify CS surfaces [32,35]. Due to the advantages over conventional methods in terms of high selectivity, clearer reaction profiles, relatively benign settings, and simplicity of handling, organic synthesis has been using a greener approach during the past few decades [37,38]. Organic scientists are concentrating on employing ultrasonic-assisted organic synthesis since it is a green method with numerous beneficial impacts in synthetic organic chemistry [11,24,39–42].

Fused pyrimidine systems, especially pyridopyrimidines, attracted organic chemists very much due to their significant biological and pharmacological activities, which include anticancer [43–45], antiviral [46], antibacterial [43,47], anti-inflammatory and antioxidant [48–51], antihistaminic [52], antitumor [53–56] and antipyretic [57]. Some examples of bioactive pyridopyrimidine compounds with pharmaceutical properties are shown in Scheme 1.

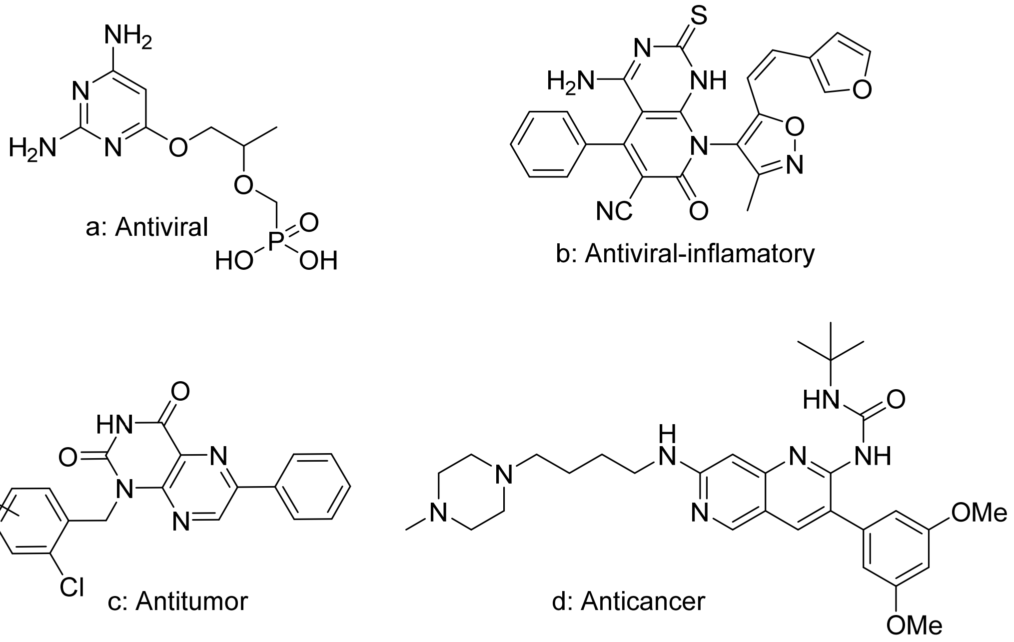

Scheme 1. The examples of bioactive pyridopyrimidine compounds with pharmaceutical properties ((**a**) [46], (**b**) [48], (**c**) [53], (**d**) [44]).

Because of its wide range of individual characteristics, this class of heterocycles is therefore of great research interest, and there is an increasing need for pyridopyrimidine nuclei to be designed and produced [14,16,58–70]. A number of approaches have been developed for the synthesis of pyridopyrimidines, where the products are designed in single- or multi-component procedures (MCRs). Due to the favorable traits, simplicity, and variety this method provides, multi-component reactions (MCRs) are more advantageous in the synthesis of pyridopyrimidines [62,71,72].

Owing to the extension of biological and pharmacological activities of pyridopyrimidines, the development of efficient, new, feasible, and environmentally friendly methods is still required. In addition, biodegradable and green catalysts are essential in modern chemical synthesis. In continuation of our previous reports with elevated interest in the heterocycle synthesis via developing effective, green, and eco-friendly procedures [10,11,14–16,73,74], we investigate a new strategy for the synthesis of pyrido[2,3-*d*] pyrimidine-dione derivatives under ultrasonic irradiation in water via superparamagnetic nanoparticle SPION@CS-IL as a novel and reusable nanocatalyst (Scheme 2). In addition, the structure of SPION@CS-IL is presented in Scheme 3.

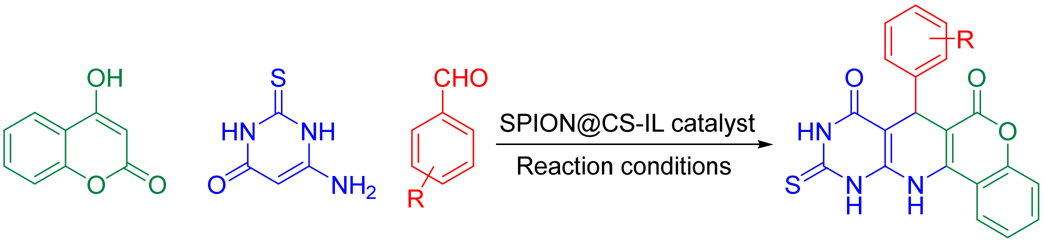

Scheme 2. Synthesis of pyrido[2,3-*d*]pyrimidine-dione derivatives **4a–j** catalyzed by SPION@CS-IL via multi-component reactions (MCRs) under ultrasonic irradiation in water.

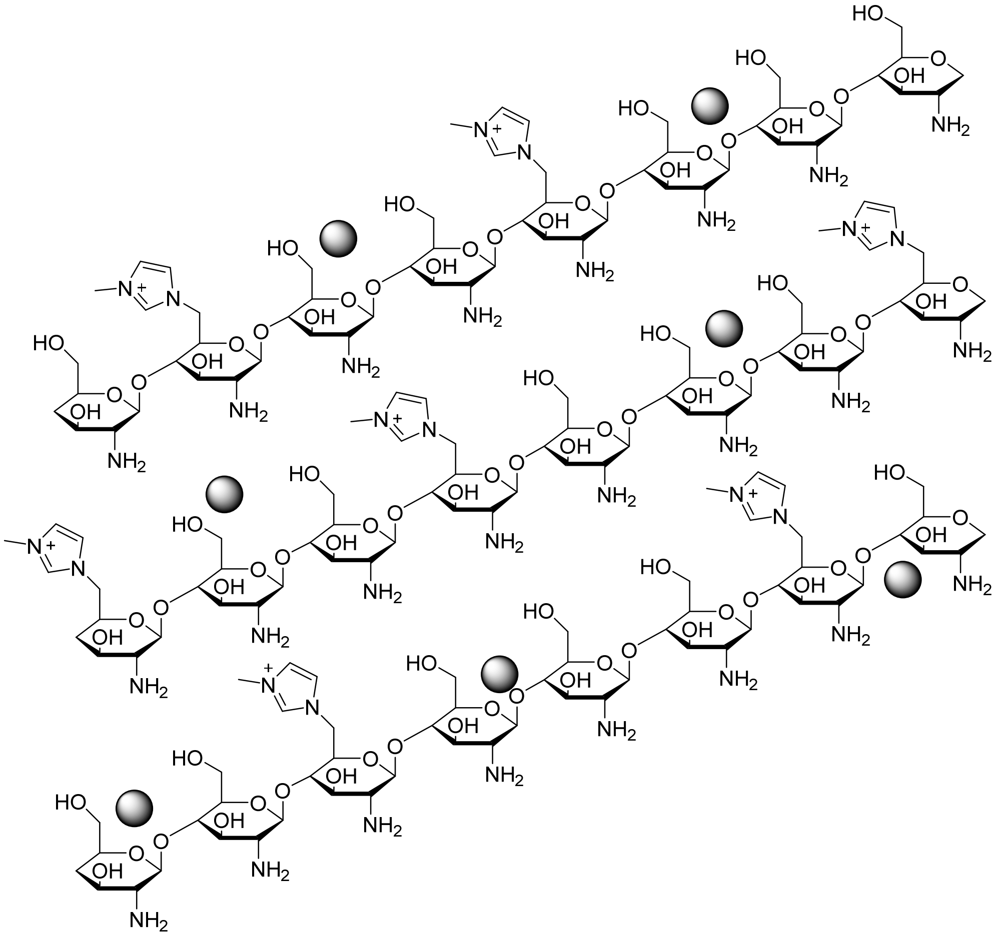

Scheme 3. A schematic structure of SPION@CS-IL catalyst.

2. Results

2.1. Characterization of SPION@CS-IL as a Heterogeneous Catalyst

In this study, a novel and reusable catalyst based on SPION@CS functionalized ionic liquid (SPION@CS-IL) was prepared and introduced as a green and reusable nanocatalyst. Superparamagnetic iron oxide nanoparticles (SPIONs) were originally created in order to accomplish this goal through the co-precipitation of Fe^{2+} and Fe^{3+} ions. The SPIONs were then functionalized with chitosan to give SPION@CS, and SPION@CS were tosylated and then react with methyl imidazole to obtain SPION@CS-IL. According to calculations based on energy dispersive X-ray analysis (EDX), the elemental compositions of SPION@CS-IL nanoparticles are 74.6%, 21.94%, 2.94%, and 0.52% for Fe, O, C, and N, respectively. This observation confirms that the chitosan was successfully modified by the superparamagnetic iron oxide nanoparticle (Figure 1).

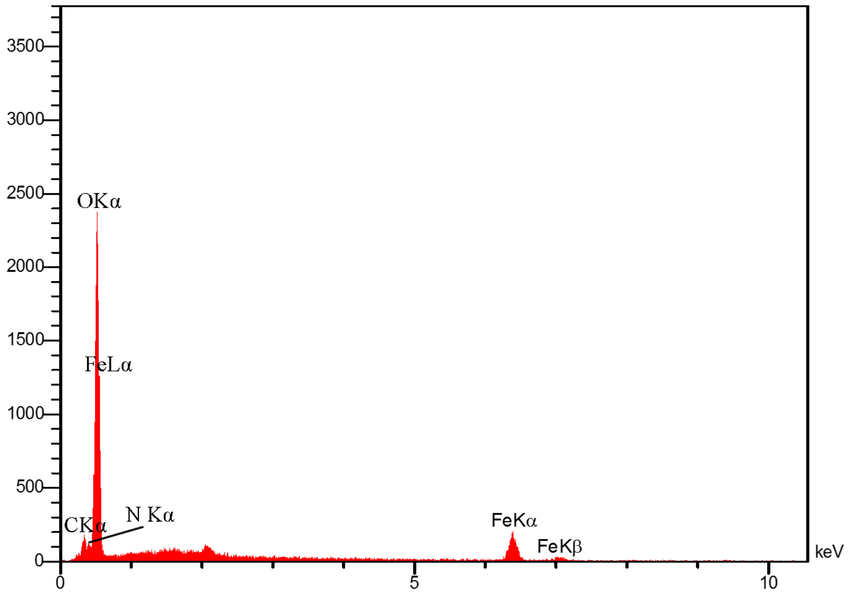

Figure 1. The energy dispersive X-ray (EDX) of SPION@CS-IL.

The successful functionalization of SPION with CS-IL was investigated using FT-IR spectroscopy. The FT-IR spectrum of SPION@CS-IL could be observed in Figure 2. Based on the result in Figure 2, specific vibrations belonging to all of the excepted functional groups in the structure of the SPION@CS-IL catalyst could be seen. The vibrations at 568 cm^{-1} could be due to the presence of Fe-O bonds in the stricture of the catalyst, which belongs to the SPIONs. In addition, the peaks at the wavenumber of 1102 cm^{-1} could be correlated to the Si-O bonds in the structure of the catalyst. Also, the vibrations of the imidazolium functionality could be seen in 1571 cm^{-1}. This peak is observed due to the C=N vibrations. Also, the vibrations of the O-H bonds are presented at the wavenumber of 3409 cm^{-1}. It should be noted that the observed band at 2930 cm^{-1} could be correlated to the aliphatic C-H vibrations that are present in the structure of the SPION@CS-IL catalyst. Regarding the FT-IR results of the SPION@CS-IL catalyst, all the expected peaks were observed in the spectrum, which confirms the successful synthesis of the SPION@CS-IL catalyst. The results are in agreement with previously reported chitosan functionalized SPION [75].

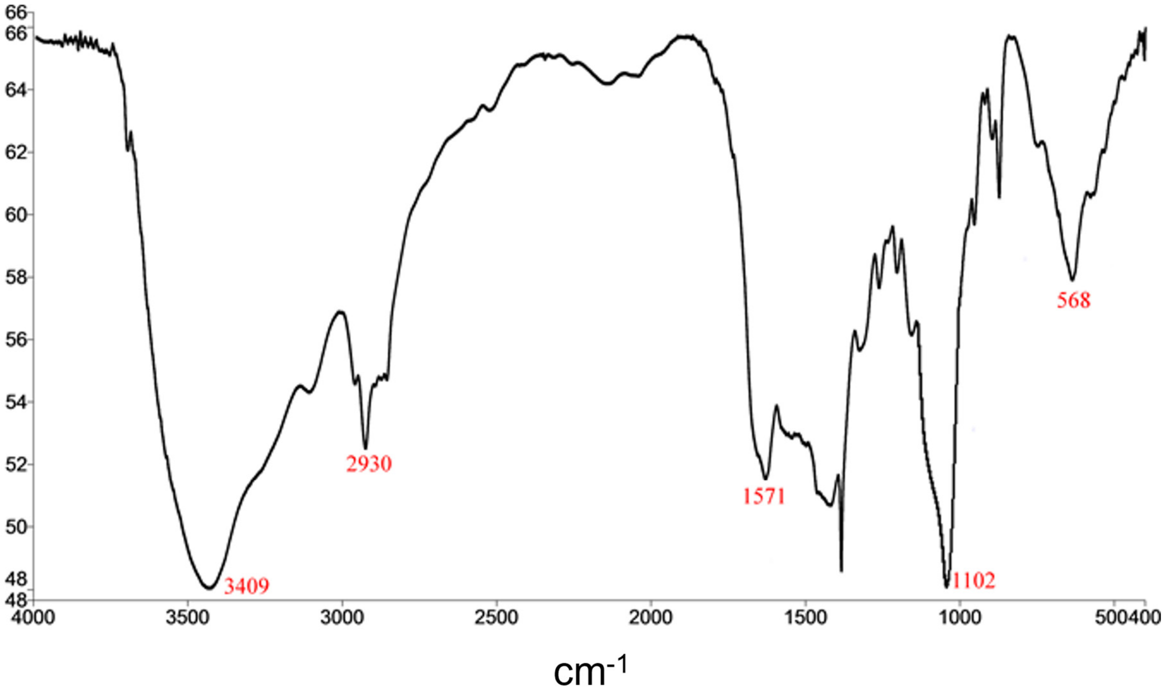

Figure 2. FT-IR spectrum of SPION@CS-IL catalyst.

The transition electron microscopy (TEM) method was used to examine the structural details of the SPION@CS-IL catalyst. Figure 3 displays the TEM images of the SPION@CS-IL catalyst. In the TEM image that is presented in Figure 3, superparamagnetic iron oxide nanoparticles can be seen as black regions. The organic groups that include chitosan and ionic liquid are shown by the lighter areas. TEM results confirm the presence of SPION on the structure of the SPION@CS-IL catalyst.

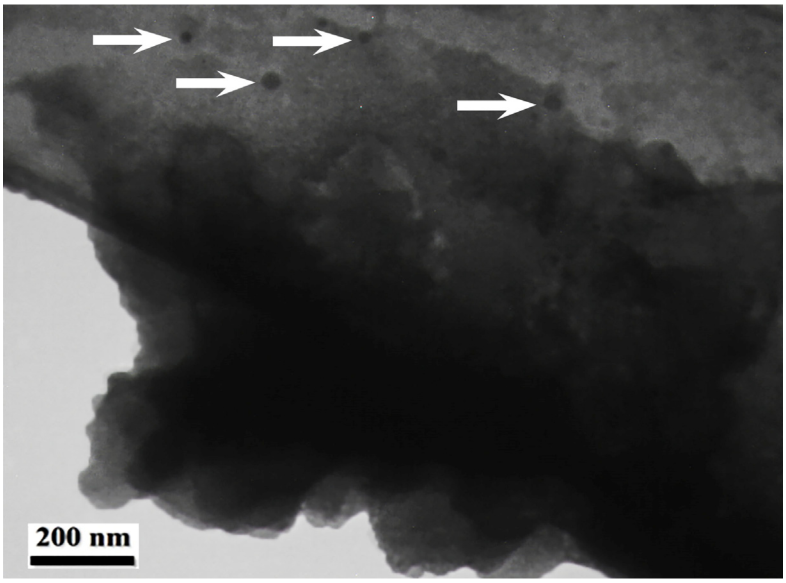

Figure 3. TEM image of SPION@CS-IL catalyst. The arrows show the SPION.

Thermogravimetric analysis (TGA) of the SPION@CS-IL was investigated to determine the thermal stability (Figure 4). The catalyst is stable below 300 °C. Due to the hydrophilic nature of ionic liquid units, the first weight loss at a low temperature of roughly 100 °C is associated with the physical adsorption of water onto the SPION@CS-IL catalyst. After that, the catalyst is thermally stable up to 250 °C. The significant weight loss is visible above 300 °C, where the disintegration of chitosan and ionic liquid begins.

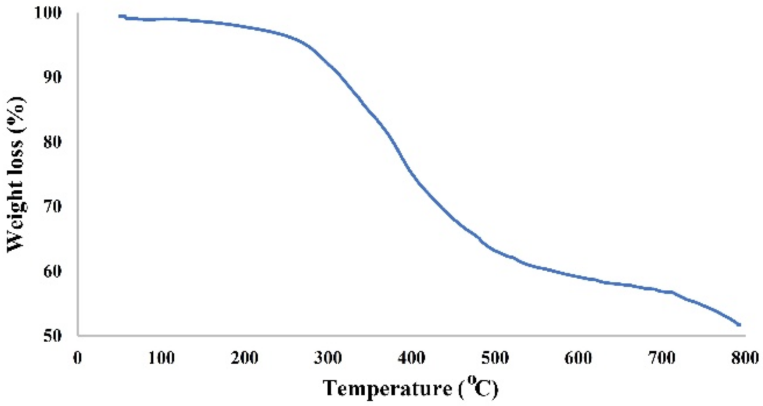

Figure 4. TGA curve of SPION@CS-IL catalyst.

The vibrating sample magnetometer (VSM) method was used to evaluate the magnetic performance of the SPION@CS-IL catalyst. The superparamagnetic behavior of the catalyst may be seen in the VSM curve, which is shown in Figure 5. These results show the saturation magnetization values for SPION (blue) and SPION@CS-IL (red), which have been 75 and 40 emu/g, respectively. These findings demonstrated that functionalizing the catalyst with CS-IL significantly reduced the magnetization of SPION. The SPION@CS-IL catalyst's magnetism is high enough to allow it to be removed from the reaction mixture using an outside magnet, though.

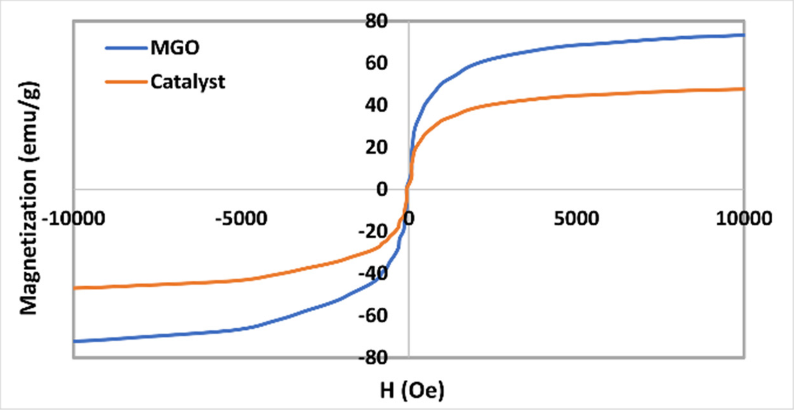

Figure 5. VSM curve of SPION and SPION@CS-IL.

2.2. Evaluation of the Catalytic Activity of SPION@CS-IL through the Synthesis of Pyrido[2,3-d] pyrimidine-dione

After SPION@CS-IL was characterized, its catalytic activity was tested in a model reaction involving the multicomponent reactions of 4-hydroxy coumarin, 6-amino-4-thioxo-3,4-dihydropyrimidin-2(1*H*)-one, and 4-nitro-benzaldehyde. In order to determine the best conditions for obtaining the largest isolated yields of the products, the reaction was carried out under a variety of reaction conditions. Table 1 displays the results of the optimization. The reaction was carried out at room temperature under ultrasonic conditions with water as the solvent, and the best-isolated yields were obtained. In addition, a good isolated yield was observed for the thermal conditions, then the reaction was performed in ethanol in the presence of 5 mg of the catalyst at 70 °C. However, a higher isolated yield was observed in the case of the reactions under ultrasonic irradiation.

Table 1. The optimization of the reaction conditions for the synthesis of **4g** (R = 4-NO_2).

Entry	Solvent	Temp (°C) [a]	Catalyst Amount (mg)	Isolated Yield (%)	
				Thermal [b]	Ultrasonic [c]
1	DMSO	70	5	31	14
2	MeOH	60	5	16	27
3	H_2O/EtOH	70	5	77	60
4	CH_2Cl_2	Reflux	5	Trace	45
5	DMF	70	5	30	32
6	H_2O	70	5	14	92
7	H_2O	50	5	Trace	Non
8	H_2O	85	5	19	Non
9	H_2O	70	Non	Non	Non
10	H_2O	70	3	Trace	73
11	H_2O	70	8	18	92
12	EtOH	70	5	89	85
13	EtOH	50	5	55	Non
14	EtOH	Reflux	5	89	Non
15	EtOH	70	Non	Non	Non
16	EtOH	70	3	66	68
17	EtOH	70	8	89	86

[a] Temperature optimization is only applied for thermal conditions. In the case of ultrasonic irradiation, the reactions were performed at room temperature. [b] reaction conditions: 4-hydroxycoumarin (1 mmol), benzaldehyde (1 mmol), 6-amino-2-thioxo-2,3-dihydropyrimidin-4(1*H*)-one (1 mmol), SPION@CS-IL (5 mg), solvent (3 mL). [c] reaction conditions: 4-hydroxycoumarin (1 mmol), benzaldehyde (1 mmol), 6-amino-2-thioxo-2,3-dihydropyrimidin-4(1*H*)-one (1 mmol), SPION@CS-IL (5 mg), solvent (5 mL), room temperature.

The universality of this catalytic system was examined by utilizing aldehydes with various derivatives once the reaction conditions had been optimized. The results are presented in Table 2. For studying the generality of the method, the reaction was performed using various substrates to synthesize different products using SPION@CS-IL catalyst. Based on the results, all the substrates have participated in the reaction to obtain the desired products in high isolated yields. As an advantage, this method is efficient in both thermal and ultrasonic-promoted conditions. In both cases, very high isolated yields are obtained. The ultrasonic reaction has the advantage of higher isolated yield and less reaction time. However, the SPION@CS-IL showed very good efficiency in both reaction conditions. The introduction of a catalyst, which is efficient and versatile in various conditions is the advantage and benefit of this work. It should be noted that the catalyst is based on a highly green and recyclable material that is achieved from shrimp shell waste.

Different aldehydes with electron withdrawing or electron donating functionalities were chosen for the synthesis of pyrido[2,3-*d*] pyrimidine-dione derivatives. Both electron-rich and electron-deficient aldehydes have given the desired products in high isolated yields under ultrasonic irradiation in short reaction times. Moreover, a significant increase in the rate and product yield was observed when the electron-withdrawing groups were replaced at the para-position of aryl aldehyde.

The reusability of this catalyst is a particularly noteworthy feature. This simple reaction approach for the separation of SPION@CS-IL has the advantage of eliminating the time-consuming workup steps for the separation and recovery of the catalyst. The catalyst can be removed from the reaction mixture utilizing an external magnet. As a model reaction to assess the catalyst's reusability, the reaction of 4-hydroxy coumarin, 6-amino-4-thioxo-3,4-dihydropyrimidin-2(1*H*)-one, and 4-nitro-benzaldehyde was used. The catalyst was separated by an external magnet after the reaction was finished and employed in the following subsequent process. The catalyst was applied in 5 separate reactions in order. Table 3 displays the reaction yield for each reaction. As demonstrated, no discernible activity reduction was seen after 5 consecutive runs.

Table 2. SPION@CS-IL -catalyzed the synthesis of pyrido[2,3-*d*] pyrimidine-dione derivatives.

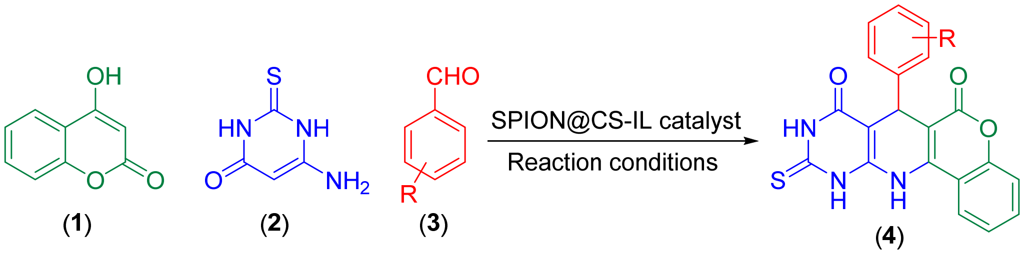

Entry	Compound	R	Isolated Yield (%)	
			Thermal [a]	Ultrasonic [b]
1	**4a**	H	85	91
2	**4b**	2-Cl	82	88
3	**4c**	3-Cl	84	89
4	**4d**	4-Cl	80	92
5	**4e**	2,4-Cl_2	77	90
6	**4f**	2-NO_2	88	91
7	**4g**	4-NO_2	89	92
8	**4h**	3-OMe	79	85
9	**4i**	4-CN	84	84
10	**4j**	4-Br	85	89

[a] reaction conditions: 4-hydroxycoumarin (1 mmol), benzaldehyde (1 mmol), 6-amino-2-thioxo-2,3-dihydropyrimidin-4(1*H*)-one (1 mmol), SPION@CS-IL (5 mg), ethanol (3 mL), 70 °C. [b] reaction conditions: 4-hydroxycoumarin (1 mmol), benzaldehyde (1 mmol), 6-amino-2-thioxo-2,3-dihydropyrimidin-4(1*H*)-one (1 mmol), SPION@CS-IL (5 mg), H_2O (5 mL), room temperature.

Table 3. The effect of reusability of SPION@CS-IL on the product **4g** yield.

Entry	Run	Isolated Yield (%)	
		Thermal [a]	Ultrasonic [b]
1	1	89	92
2	2	87	92
3	3	86	91
4	4	84	90
5	5	83	90

[a] reaction conditions: 4-hydroxycoumarin (1 mmol), benzaldehyde (1 mmol), 6-amino-2-thioxo-2,3-dihydropyrimidin-4(1*H*)-one (1 mmol), SPION@CS-IL (5 mg), ethanol (3 mL), 70 °C. [b] reaction conditions: 4-hydroxycoumarin (1 mmol), benzaldehyde (1 mmol), 6-amino-2-thioxo-2,3-dihydropyrimidin-4(1*H*)-one (1 mmol), SPION@CS-IL (5 mg), H_2O (5 mL), room temperature.

In reaction conditions, the catalyst must keep its chemical and physical properties. The effectiveness and recovery of the reaction depend on the catalyst's stability. After the fifth reaction run, the catalyst was removed from the reaction and washed with ethanol before being cleaned with a 0.1 M aqueous solution of hydrochloric acid to remove any potential impurities from the catalyst's surface. This was performed in order to study the stability of the SPION@CS-IL catalyst. After the fifth reaction run, the SPION@CS-IL catalyst's microstructure was assessed by TEM analysis. Figure 6 displays the TEM picture of SPION@CS-IL following the catalyst's recovery. As it demonstrates, the catalyst's structure has been preserved under the reaction circumstances. It should be noted that the catalyst showed very good dispersion in the reaction mixture during the reaction. On the other hand, after the reaction completion, SPION@CS-IL was easily separated from the reaction mixture using an external magnet.

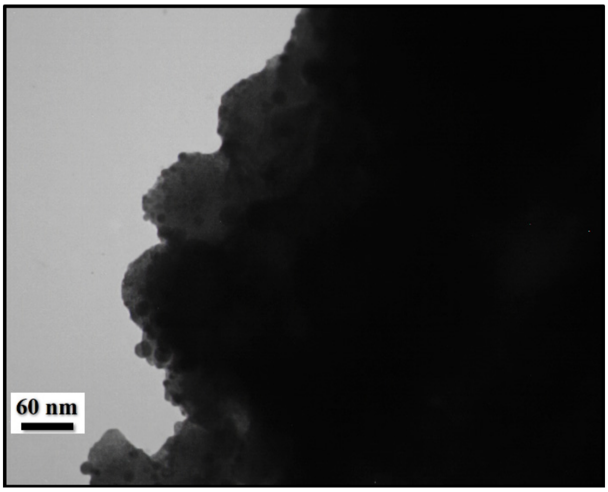

Figure 6. TEM image of SPION@CS-IL after the fifth run.

3. Materials and Methods

3.1. Chemical and Apparatus

All the chemicals, reagents, and solvents were purchased from Sigma, Merck, Fluka, and Aldrich. Products were characterized by their physical constant and comparison with authentic samples. Reaction monitoring was accomplished by TLC on silica gel polygram SILG/UV 254 plates. FT-IR spectra were recorded on a Shimadzu FT-IR 550 spectrometer using KBr disks to detect content variations of the functional groups. ^{1}H and ^{13}C NMR spectra were recorded in DMSO-d$_6$ on a Bruker 250 MHz spectrometer using TMS as the internal standard. Mass spectra of the samples were recorded on an Agilent Technology (HP) mass spectrometer operating at an ionization potential of 70 eV. Elemental analysis was accomplished with an elementary analysen system GmbH VarioEL CHNS mode. Thermogravimetric analysis (TGA) of nanocatalyst was performed at a heating rate of 10 °C min^{-1} over the temperature range of 40–600 °C under a nitrogen atmosphere ((TGA, PerkinElmer, Pyris 1, USA). For examining the crystal structure of nanoparticles, an X-ray powder diffraction (XRD) diffractometer (Cu Ka, radiation, λ = 1.5405 Å) was run at a scanning speed of 2/min from 10 to 80 (2θ). To discover the magnetic properties of the nanoparticles, a vibrating sample magnetometer. (VSM, model BHV-55, Riken, Japan) the experiment was run with a magnetic field up to 10 kOe. The morphology and particle size of nanoparticles were obtained via transmission electron microscopy (TEM) operating with a Leo 912 AB at an accelerating voltage of 200 kV. Compositional analysis of nanocatalysts was obtained by X-ray energy dispersive spectroscopy (EDX).

3.2. Synthesis of SPION@CS

For the synthesis of SPION@CS, magnetic nanoparticles coated with silica were first prepared according to the previously reported procedure [76] SPION coated with silica (1.0 g) were added to a round bottom flask containing 25 mL of thionyl chloride and sonicated for 30 min. The mixture was then stirred under reflux conditions under an argon atmosphere. After the reaction time, the mixture was cooled to room temperature and the solid was isolated by a magnet. In a flask containing the solid product, was added 25 mL of chloroform and sonicated for 30 min. To the above mixture was added chitosan (1.0 g) and triethylamine (0.5 mL) and refluxed overnight. The product was separated and washed by chloroform (3 × 10 mL) and water (3 × 10 mL) for the neutralization of any possible unreacted chlorosilyl groups on the surface of the magnetic nanoparticles. The SPION@CS was dried in a vacuum oven overnight.

3.3. Synthesis of Tosylated SPION@CS

Tosylated SPION@CS was prepared by the reaction of SPION@CS and 4-toluenesulfonyl chloride. For this purpose, SPION@CS (5.65 g, 5 mmol) was dissolved in deionized water (30 mL) and NaOH (10 mmol) was added. The mixture was stirred for 15 min at room temperature and then a solution of 4-toluenesulfonyl chloride (1.43 g, 7.5 mmol) in 20 mL of acetonitrile was added dropwise for 30 min. The mixture was stirred under an argon atmosphere for 6 h. The product was separated by a magnet and washed with an ammonium chloride solution until the pH was between 7 and 8.

3.4. Synthesis of SPION@CS-IL

Methyl imidazole (3 mmol) was added to the dispersed tosylated SPION@CS (3 mmol) in dry DMF (20 mL) and stirred for 24 h at 80 °C under an argon atmosphere. The reaction was cooled to room temperature after 24 h, and SPION@CS-IL was separated by a magnet and washed with acetone (3 × 10 mL). The product was dried in a vacuum oven overnight.

3.5. General Procedure for the Synthesis of Pyrido[2,3-d]pyrimidine-dione Derivatives over SPION@CS-IL Catalyst in the Solvent under Reflux

4-hydroxycoumarin (1 mmol), benzaldehyde (1 mmol), and 6-amino-2-thioxo-2,3-dihydropyrimidin-4(1*H*)-one (1 mmol) were added into a flask containing ethanol (3 mL). A total of 5 mg of SPION@CS-IL was added and the reaction mixture was stirred for 24 h at 70 °C. The reaction performance was followed up by thin layer chromatography, hexane/ethyl acetate, 95:5, volume ratio and after the reaction was completed, the catalyst was separated from the reaction mixture. The product was purified by recrystallization from ethanol and characterized by ^{1}H NMR, ^{13}C NMR, MS, FTIR, and melting point.

3.6. General Procedure for the Synthesis of Pyrido[2,3-d]pyrimidine-dione Derivatives over SPION@CS-IL Catalyst under Ultrasonic Irradiation in Water

4-hydroxycoumarin (1 mmol), benzaldehyde (1 mmol), 6-amino-2-thioxo-2,3-dihydropyrimidin-4(1*H*)-one (1 mmol), and SPION@CS-IL catalyst (5 mg) were added to a vessel containing 5 mL of distilled water. An ultrasonic probe was placed into the reaction mixture and sonicated for an appropriate time. The catalyst was separated from the reaction mixture and the solvent was evaporated after the completion of the reaction (monitored by thin later chromatography, hexane/ethyl acetate, 95:5, volume ratio). The products were recrystallized from ethanol to give the pure product and characterized by ^{1}H NMR, ^{13}C NMR, MS, FTIR, and melting point.

4. Conclusions

We have developed a novel and reusable superparamagnetic iron oxide nanoparticles@Chitosan functionalized ionic liquid (SPION@CS-IL) as a reusable heterogeneous superparamagnetic catalyst for green one-pot synthesis of pyrido[2,3-*d*]pyrimidine-dione derivatives using a direct three-component reaction method of thiobarbituric acid, 4-hydroxy coumarin, and different aromatic aldehydes, under ultrasonic irradiation as an eco-friendly method in water as a "green" solvent. A variety of techniques are used to fully characterize the catalyst, including FT-IR, XRD, EDX, TEM, VSM, and TGA. All of the products were successfully synthesized with excellent isolated yields. Filtration made it simple to separate the catalyst from the products, and it also demonstrates significant reusable activity (5 runs). Shorter reaction times, low catalyst loadings, the nanocatalyst's capacity to be recycled five times, and the absence of harmful chemical reagents are all significant advantages of this environmentally benign process. As an advantage, chitosan that is used as a support for the catalyst is obtained from a natural resource. In addition, SPION@CS-IL catalyst shows very good separation from the reaction mixture using an external magnet due to the magnetic properties of SPION. The high activity of SPION@CS-IL is proved in the one-pot synthesis of pyrido[2,3-*d*]pyrimidinedione derivatives.

Author Contributions: M.H.S., A.S. and F.B. performed the experiments. M.H.S., M.M. and S.B. analyzed the data. F.D., M.M. and S.B. prepared the manuscript. M.H.S. and S.B. led the work. All authors have read and agreed to the published version of the manuscript.

Funding: This research received no external funding.

Data Availability Statement: The data presented in this study are available in this article.

Conflicts of Interest: The authors declare no conflict of interest.

References

1. Li, A.Y.; Moores, A. Carbonyl reduction and biomass: A case study of sustainable catalysis. *ACS Sustain. Chem. Eng.* **2019**, *7*, 10182–10197. [CrossRef]
2. Hutchings, G.J. Heterogeneous gold catalysis. *ACS Cent. Sci.* **2018**, *4*, 1095–1101. [CrossRef] [PubMed]
3. Anastas, P.T.; Kirchhoff, M.M.; Williamson, T.C. Catalysis as a foundational pillar of green chemistry. *Appl. Catal. A Gen.* **2001**, *221*, 3–13. [CrossRef]
4. Centi, G.; Perathoner, S. Catalysis: Role and challenges for a sustainable energy. *Top. Catal.* **2009**, *52*, 948–961. [CrossRef]
5. Lamb, A.C.; Lee, A.F.; Wilson, K. Recent Advances in Heterogeneous Catalyst Design for Biorefining. *Aust. J. Chem.* **2020**, *73*, 832–852. [CrossRef]
6. Yang, C.; Wu, J.; Hou, Y. Fe_3O_4 nanostructures: Synthesis, growth mechanism, properties and applications. *Chem. Commun.* **2011**, *47*, 5130–5141. [CrossRef]
7. Xu, C.; Sun, S. Superparamagnetic nanoparticles as targeted probes for diagnostic and therapeutic applications. *Dalton. Trans.* **2009**, *29*, 5583–5591. [CrossRef]
8. Samanta, A.; Ravoo, B.J. Magnetic Separation of Proteins by a Self-Assembled Supramolecular Ternary Complex. *Angew. Chem. Int. Ed.* **2014**, *53*, 12946–12950. [CrossRef]
9. Xu, L.; Kim, M.J.; Kim, K.D.; Choa, Y.H.; Kim, H.T. Surface modified Fe_3O_4 nanoparticles as a protein delivery vehicle. *Colloids Surf. A Physicochem. Eng. Asp.* **2009**, *350*, 8–12. [CrossRef]
10. Dehghani, F.; Sardarian, A.R.; Esmaeilpour, M. Salen complex of Cu(II) supported on superparamagnetic Fe_3O_4@SiO_2 nanoparticles: An efficient and recyclable catalyst for synthesis of 1- and 5-substituted-1*H*-tetrazoles. *J. Organomet. Chem.* **2013**, *743*, 87–96. [CrossRef]
11. Esmaeilpour, M.; Javidi, J.; Dehghani, F.; Nowroozi Dodeji, F. A green one-pot three-component synthesis of tetrahydrobenzo[*b*]pyran and 3,4-dihydropyrano[*c*]chromene derivatives using a Fe_3O_4@SiO_2-imid-PMA; magnetic nanocatalys. *RSC Adv.* **2015**, *5*, 26625–26633. [CrossRef]
12. Bahadorikhalili, S.; Ashtari, A.; Ma'mani, L.; Ranjbar, P.R.; Mahdavi, M. Copper-supported β-cyclodextrin-functionalized magnetic nanoparticles: Efficient multifunctional catalyst for one-pot 'green' synthesis of 1,2,3-triazolylquinazolinone derivatives. *Appl. Organomet. Chem.* **2018**, *32*, e4212. [CrossRef]
13. Bahadorikhalili, S.; Mahdavi, M.; Ma'mani, L.; Shafiee, A.; Mahdavi, H.; Akbarzadeh, T. Palladium functionalized phosphinite polyethyleneimine grafted magnetic silica nanoparticles as an efficient catalyst for the synthesis of isoquinolino[1,2-*b*]quinazolin-8-ones. *New J. Chem.* **2018**, *42*, 5499–5507. [CrossRef]
14. Sayahi, M.H.; Shamkhani, F.; Mahdavi, M.; Bahadorikhalili, S. Sulfonic Acid Functionalized Magnetic Starch as an Efficient Catalyst for the Synthesis of Chromeno[4,3-*b*]quinoline-6,8(9*H*)-dione Derivatives. *Starch-Stärke* **2021**, *73*, 2000257. [CrossRef]
15. Tashrifi, Z.; Bahadorikhalili, S.; Lijan, H.; Ansari, S.; Hamedifar, H.; Mahdavi, M. Synthesis and characterization of γ-Fe_2O_3@SiO_2-$(CH_2)_3$-PDTC-Pd magnetic nanoparticles: A new and highly active catalyst for the Heck/Sonogashira coupling reactions. *New J. Chem.* **2019**, *43*, 8930–8938. [CrossRef]
16. Sayahi, M.H.; Bahadorikhalili, S.; Saghanezhad, S.J.; Miller, M.A.; Mahdavi, M. Sulfonic acid-functionalized poly(4-styrenesulfonic acid) mesoporous graphene oxide hybrid for one-pot preparation of coumarin-based pyrido[2,3-*d*]pyrimidine-dione derivatives. *Res. Chem. Intermed.* **2020**, *46*, 491–507. [CrossRef]
17. Lee, Y.; Kang, I. Optimal Fabrication Conditions of Chitosan-Fe_3O_4-Gold Nanoshells as an Anticancer Drug Delivery Carriers. *Bull. Korean Chem. Soc.* **2017**, *38*, 313–319. [CrossRef]
18. Zhao, L.; Liu, H.; Wang, F.; Zeng, L. Design of yolk-shell Fe_3O_4@PMAA composite microspheres for adsorption of metal ions and pH-controlled drug delivery. *J. Mater. Chem. A* **2014**, *2*, 7065–7074. [CrossRef]
19. Guo, Z.; Li, Y.; Pan, S.; Xu, J. Fabrication of Fe_3O_4@cyclodextrin magnetic composite for the high-efficient removal of Eu (III). *J. Mol. Liq.* **2015**, *206*, 272–277. [CrossRef]
20. Cristofanilli, M.; Hayes, D.F.; Budd, G.T.; Ellis, M.J.; Stopeck, A.; Reuben, J.M.; Doyle, G.V.; Matera, J.; Allard, W.J.; Miller, M.C.; et al. Circulating tumor cells: A novel prognostic factor for newly diagnosed metastatic breast cancer. *J. Clin. Oncol.* **2005**, *23*, 1420–1430. [CrossRef]
21. Tran, H.V.; Dai Tran, L.; Nguyen, T.N. Preparation of chitosan/magnetite composite beads and their application for removal of Pb(II) and Ni(II) from aqueous solution. *Mater. Sci. Eng. C* **2010**, *30*, 304–310. [CrossRef] [PubMed]
22. Dai Tran, L.; Nguyen, B.H.; Van Hieu, N.; Tran, H.V.; Le Nguyen, H.; Nguyen, P.X. Electrochemical detection of short HIV sequences on chitosan/Fe3O4 nanoparticle based screen printed electrodes. *Mater. Sci. Eng. C* **2011**, *31*, 477–485. [CrossRef]

23. Naghipour, A.; Fakhri, A. Efficient oxidation of sulfides into sulfoxides catalyzed by a chitosan-Schiff base complex of Cu(II) supported on supramagnetic Fe_3O_4 nanoparticles. *Environ. Chem. Lett.* **2016**, *14*, 207–213. [CrossRef]
24. Safari, J.; Javadian, L. Ultrasound assisted the green synthesis of 2-amino-4*H*-chromene derivatives catalyzed by Fe_3O_4-functionalized nanoparticles with chitosan as a novel and reusable magnetic catalyst. *Ultrason. Sonochem.* **2015**, *22*, 341–348. [CrossRef] [PubMed]
25. Bandi, S.; Hastak, V.; Pavithra, C.L.; Kashyap, S.; Singh, D.K.; Luqman, S.; Peshwe, D.R.; Srivastav, A.K. Graphene/chitosan-functionalized iron oxide nanoparticles for biomedical applications. *J. Mater. Res.* **2019**, *34*, 3389–3399. [CrossRef]
26. Azizi, K.; Esfandiary, N.; Karimi, M.; Yazdani, E.; Heydari, A. Imidazolium chloride immobilized on copper acetylacetonate-grafted magnetic chitosan as a new metal/ionic liquid bifunctional catalyst for selective oxidation of benzyl alcohols in water. *RSC Adv.* **2016**, *6*, 89313–89321. [CrossRef]
27. Rakhtshah, J.; Yaghoobi, F. Catalytic application of new manganese Schiff-base complex immobilized on chitosan-coated magnetic nanoparticles for one-pot synthesis of 3-iminoaryl-imidazo[1,2-*a*]pyridines. *Int. J. Biol. Macromol.* **2019**, *139*, 904–916. [CrossRef] [PubMed]
28. Mousavi, H. A comprehensive survey upon diverse and prolific applications of chitosan-based catalytic systems in one-pot multi-component synthesis of heterocyclic rings. *Int. J. Biol. Macromol.* **2021**, *186*, 1003–1166. [CrossRef]
29. Safari, J.; Azizi, F.; Sadeghi, M. Chitosan nanoparticles as a green and renewable catalyst in the synthesis of 1,4-dihydropyridine under solvent-free conditions. *New J. Chem.* **2015**, *39*, 1905–1909. [CrossRef]
30. Safari, J.; Tavakoli, M.; Ghasemzadeh, M.A. A highly effective synthesis of pyrimido[4,5-*b*]quinoline-tetraones using $H_3PW_{12}O_{40}$/chitosan/$NiCo_2O_4$ as a novel magnetic nanocomposite. *Polyhedron* **2020**, *182*, 114459. [CrossRef]
31. Mahé, O.; Brière, J.F.; Dez, I. Chitosan: An upgraded polysaccharide waste for organocatalysis. *Eur. J. Org. Chem.* **2015**, *2015*, 2559–2578. [CrossRef]
32. Sun, J.; Wang, J.; Cheng, W.; Zhang, J.; Li, X.; Zhang, S.; She, Y. Chitosan functionalized ionic liquid as a recyclable biopolymer-supported catalyst for cycloaddition of CO_2. *Green Chem.* **2012**, *14*, 654–660. [CrossRef]
33. Safari, J.; Zarnegar, Z.; Sadeghi, M.; Azizi, F. Chitosan-SO_3H: An Efficient and Biodegradable Catalyst for the Green Syntheses of 1,4-dihydropyridines. *Curr. Org. Chem.* **2016**, *20*, 2926–2932. [CrossRef]
34. Chtchigrovsky, M.; Primo, A.; Gonzalez, P.; Molvinger, K.; Robitzer, M.; Quignard, F.; Taran, F. Functionalized chitosan as a green, recyclable, biopolymer-supported catalyst for the [3+2] huisgen cycloaddition. *Angew. Chem. Int. Ed.* **2009**, *48*, 5916–5920. [CrossRef] [PubMed]
35. Wei, Y.; Huang, W.; Zhou, Y.; Zhang, S.; Hua, D.; Zhu, X. Modification of chitosan with carboxyl-functionalized ionic liquid for anion adsorption. *Int. J. Biol. Macromol.* **2013**, *62*, 365–369. [CrossRef]
36. Ayati, A.; Daraie, M.; Heravi, M.M.; Tanhaei, B. $H_4[W_{12}SiO_{40}]$ grafted on magnetic chitosan: A green nanocatalyst for the synthesis of [1,2,4]triazolo/benzimidazolo quinazolinone derivatives. *Micro Nano Lett.* **2017**, *12*, 964–969. [CrossRef]
37. Zang, H.; Wang, M.; Cheng, B.-W.; Song, J. Ultrasound-promoted synthesis of oximes catalyzed by a basic ionic liquid [bmIm] OH. *Ultrason. Sonochem.* **2009**, *16*, 301–303. [CrossRef]
38. Riadi, Y. Green, rapid and efficient synthesis of new antibacterial pyridopyrimidinone mediated by eutectic mixture of Urea/$CuCl_2$. *Sustain. Chem. Pharm.* **2020**, *15*, 100233. [CrossRef]
39. Esmaeilpour, M.; Javidi, J.; Dehghani, F.; Zahmatkesh, S. One-pot synthesis of multisubstituted imidazoles catalyzed by Dendrimer-PWAnnanoparticles under solvent-free conditions and ultrasonic irradiation. *Res. Chem. Intermed.* **2017**, *43*, 163–185. [CrossRef]
40. Mamaghani, M.; Tabatabaeian, K.; Araghi, R.; Fallah, A.; Hossein Nia, R. An Efficient, Clean, and Catalyst-Free Synthesis of Fused Pyrimidines Using Sonochemistry. *Org. Chem. Int.* **2014**, *2014*, 1–9. [CrossRef]
41. Atarod, M.; Safari, J.; Tebyanian, H. Ultrasound irradiation and green synthesized CuO-NiO-ZnO mixed metal oxide: An efficient sono/nano-catalytic system toward a regioselective synthesis of 1-aryl-5-amino-1*H*-tetrazoles. *Synth. Commun.* **2020**, *50*, 1993–2006. [CrossRef]
42. Elyasi, Z.; Ghomi, J.S.; Najafi, G.R. Ultrasound-Engineered fabrication of immobilized molybdenum complex on Cross-Linked poly (Ionic Liquid) as a new acidic catalyst for the regioselective synthesis of pharmaceutical polysubstituted spiro compounds. *Ultrason. Sonochem.* **2021**, *75*, 105614. [CrossRef] [PubMed]
43. Kahriman, N.; Peker, K.; Serdaroğlu, V.; Aydın, A.; Usta, A.; Fandaklı, S.; Yaylı, N. Novel 2-amino-4-aryl-6-pyridopyrimidines and N-alkyl derivatives: Synthesis, characterization and investigation of anticancer, antibacterial activities and DNA/BSA binding affinities. *Bioorg. Chem.* **2020**, *99*, 103805. [CrossRef]
44. Modi, S.J.; Modh, D.H.; Kulkarni, V.M. Insights into the structural features of anticancer 1,6-naphthyridines and pyridopyrimidines as VEGFR-2 inhibitors: 3D-QSAR study. *J. Appl. Pharm. Sci.* **2020**, *10*, 1–22.
45. Yadav, P.; Shah, K. An overview on synthetic and pharmaceutical prospective of pyrido[2,3-*d*]pyrimidines scaffold. *Chem. Biol. Drug. Des.* **2021**, *97*, 633–648. [CrossRef]
46. Holý, A.; Votruba, I.; Masojídková, M.; Andrei, G.; Snoeck, R.; Naesens, L.; De Clercq, E.; Balzarini, J. 6-[2-(Phosphonomethoxy) alkoxy]pyrimidines with Antiviral Activity. *J. Med. Chem.* **2002**, *45*, 1918–1929. [CrossRef]
47. Panchabhai, V.; Ingole, P.G.; Butle, S.R. Design, Synthesis and Antibacterial Studies of Some New Pyridopyrimidine Derivatives as Biotin Carboxylase Inhibitors. *Bull. Fac. Pharm. Cairo Univ.* **2020**, *58*, 40–52. [CrossRef]

48. Dasari, S.R.; Tondepu, S.; Vadali, L.R.; Seelam, N. PEG-400 mediated an efficient eco-friendly synthesis of new isoxazolyl pyrido[2,3-*d*]pyrimidines and their anti-inflammatory and analgesic activity. *Synth. Commun.* **2020**, *50*, 2950–2961. [CrossRef]
49. Rani, N.V.; Kunta, R. PEG-400 promoted a simple, efficient and eco-friendly synthesis of functionalized novel isoxazolyl pyrido[2,3-*d*]pyrimidines and their antimicrobial and anti-inflammatory activity. *Synth. Commun.* **2021**, *51*, 1171–1183. [CrossRef]
50. Zarandi, M.; Panahi, M.; Rafiee, A. Simulation of a natural gas-to-liquid process with a multitubular fischer-tropsch reactor and variable chain growth factor for product distribution. *Ind. Eng. Chem. Res.* **2020**, *59*, 19322–19333. [CrossRef]
51. Madar, J.M.; Shastri, L.A.; Shastri, S.L.; Holiyachi, M.; Naik, N.; Kulkarni, R.; Shaikh, F.; Sungar, V. Design, synthesis, characterization, and biological evaluation of pyrido[1,2-*a*]pyrimidinone coumarins as promising anti-inflammatory agents. *Synth. Commun.* **2018**, *48*, 375–386. [CrossRef]
52. Quintela, J.; Peinador, C.; Botana, L.; Estévez, M.; Riguera, R. Synthesis and antihistaminic activity of 2-guanadino-3-cyanopyridines and pyrido [2,3-*d*]-pyrimidines. *Bioorg. Med. Chem.* **1997**, *5*, 1543–1553. [CrossRef] [PubMed]
53. El-Kalyoubi, S.; Agili, F. Synthesis, in Silico Prediction and in Vitro Evaluation of Antitumor Activities of Novel Pyrido[2,3-*d*]pyrimidine, Xanthine and Lumazine Derivatives. *Molecules* **2020**, *25*, 5205. [CrossRef] [PubMed]
54. El-Hag, F.A.A.; Abdel-Hafez, N.A.; Abbas, E.M.H.; El-Manawaty, M.A.; El-Rashedy, A.A. Synthesis and Antitumor Activity of Some New Fused Heterocyclic Compounds. *Russ. J. Gen. Chem.* **2019**, *89*, 128–137. [CrossRef]
55. Aref, M.M.A. Synthesis of Some Pyridopyrimidine Derivatives of Potential Antitumor Activity. Cairo University Theses, 2018. Available online: http://erepository.cu.edu.eg/index.php/cutheses/article/view/7995 (accessed on 13 October 2022).
56. Behalo, M.S.; Mele, G. Synthesis and Evaluation of Pyrido[2,3-*d*]pyrimidine and 1,8-Naphthyridine Derivatives as Potential Antitumor Agents. *J. Heterocycl. Chem.* **2017**, *54*, 295–300. [CrossRef]
57. El-Sharkawy, K.A.; AlBratty, M.M.; Alhazmi, H.A. Synthesis of some novel pyrimidine, thiophene, coumarin, pyridine and pyrrole derivatives and their biological evaluation as analgesic, antipyretic and anti-inflammatory agents. *Braz. J. Pharm. Sci.* **2019**, *54*, 1–13. [CrossRef]
58. Chaghari-Farahani, F.; Abdolmohammadi, S.; Kia-Kojoori, R. A PANI-Fe_3O_4@ZnO nanocomposite: A magnetically separable and applicable catalyst for the synthesis of chromeno-pyrido[*d*]pyrimidine derivatives. *RSC Adv.* **2020**, *10*, 15614–15621. [CrossRef]
59. Jadhav, C.; Nipate, A.; Chate, A.; Gill, C. Triethylammonium Hydrogen Sulfate [Et_3NH][HSO_4]-Catalyzed Rapid and Efficient Multicomponent Synthesis of Pyrido[2,3-*d*]pyrimidine and Pyrazolo[3,4-*b*]pyridine Hybrids. *ACS Omega* **2021**, *6*, 18215–18225. [CrossRef]
60. Jolodar, O.G.; Shirini, F.; Seddighi, M. Efficient synthesis of pyrano[2,3-*d*]pyrimidinone and pyrido[2,3-*d*]pyrimidine derivatives in presence of novel basic ionic liquid catalyst. *Chin. J. Catal.* **2017**, *38*, 1245–1251. [CrossRef]
61. Moavi, J.; Buazar, F.; Sayahi, M.H. Algal magnetic nickel oxide nanocatalyst in accelerated synthesis of pyridopyrimidine derivatives. *Sci. Rep.* **2021**, *11*, 1–14. [CrossRef]
62. Mamaghani, M.; Hossein Nia, R. Recent Developments in the MCRs Synthesis of Pyridopyrimidines and Spiro-Pyridopyrimidines. *J. Heterocycl. Chem.* **2017**, *54*, 1700–1722. [CrossRef]
63. Zhang, F.; Li, C.; Liang, X. Solid acid-catalyzed domino cyclization reaction: Regio-and diastereoselective synthesis of pyrido[2,3-*d*]pyrimidine derivatives bearing three contiguous stereocenters. *Green Chem.* **2018**, *20*, 2057–2063. [CrossRef]
64. El Sayed, M.T.; Hussein, H.A.; Elebiary, N.M.; Hassan, G.S.; Elmessery, S.M.; Elsheakh, A.R.; Nayel, M.; Abdel-Aziz, H.A. Tyrosine kinase inhibition effects of novel Pyrazolo[1,5-*a*]pyrimidines and Pyrido[2,3-*d*]pyrimidines ligand: Synthesis, biological screening and molecular modeling studies. *Bioorg. Chem.* **2018**, *78*, 312–323. [CrossRef] [PubMed]
65. Nurjamal, K.; Brahmachari, G. Sodium Formate-Catalyzed One-Pot Synthesis of Functionalized Spiro[indoline-3,5′-pyrido[2,3-*d*]pyrimidine]/Spiro[acenaphthylene-1,5′-pyrido[2,3-*d*]-pyrimidine] Derivatives. *ChemistrySelect* **2019**, *4*, 2363–2367. [CrossRef]
66. Chandrasekaran, B.; Deb, P.K.; Kachler, S.; Akkinepalli, R.R.; Mailavaram, R.; Klotz, K.N. Synthesis and adenosine receptors binding studies of new fluorinated analogues of pyrido[2,3-*d*]pyrimidines and quinazolines. *Med. Chem. Res.* **2018**, *27*, 756–767. [CrossRef]
67. Veeraswamy, B.; Madhu, D.; Dev, G.J.; Poornachandra, Y.; Kumar, G.S.; Kumar, C.G.; Narsaiah, B. Studies on synthesis of novel pyrido[2,3-*d*]pyrimidine derivatives, evaluation of their antimicrobial activity and molecular docking. *Bioorg. Med. Chem. Lett.* **2018**, *28*, 1670–1675. [CrossRef]
68. Farahmand, T.; Hashemian, S.; Sheibani, A. Efficient one-pot synthesis of pyrano[2,3-*d*]pyrimidinone and pyrido[2,3-*d*]pyrimidine derivatives by using of Mn-ZIF-8@$ZnTiO_3$ nanocatalyst. *J. Mol. Struct.* **2020**, *1206*, 127667. [CrossRef]
69. Jalili, F.; Zarei, M.; Zolfigol, M.A.; Rostamnia, S.; Moosavi-Zare, A.R. SBA-15/PrN $(CH_2PO_3H_2)_2$ as a novel and efficient mesoporous solid acid catalyst with phosphorous acid tags and its application on the synthesis of new pyrimido[4,5-*b*]quinolones and pyrido[2,3-*d*]pyrimidines via anomeric based oxidation. *Microporous Mesoporous Mater.* **2020**, *294*, 109865. [CrossRef]
70. Jahanshahi, P.; Mamaghani, M.; Haghbin, F.; Nia, R.H.; Rassa, M. One-pot chemoselective synthesis of novel pyrrole-substituted pyrido[2,3-*d*]pyrimidines using [γ-Fe_2O_3@HAp-SO_3H] as an efficient nanocatalyst. *J. Mol. Struct.* **2018**, *1155*, 520–529. [CrossRef]
71. Herrera, R.P.; Marqués-López, E. *Multicomponent Reactions: Concepts and Applications for Design and Synthesis*; John Wiley & Sons: Hoboken, NJ, USA, 2015.
72. Cioc, R.C.; Ruijter, E.; Orru, R.V.A. Multicomponent reactions: Advanced tools for sustainable organic synthesis. *Green Chem.* **2014**, *16*, 2958–2975. [CrossRef]

73. Sayahi, M.H.; Shamkhani, F.; Mahdavi, M.; Bahadorikhalili, S. Efficient synthesis of chromeno[4,3-*b*]pyrano[3,4-*e*]pyridine-6,8-dione derivatives via multicomponent one-pot reaction under mild reaction conditions in water. *Res. Chem. Intermed.* **2021**, *47*, 4101–4112. [CrossRef]
74. Sayahi, M.H.; Afrouzandeh, Z.; Bahadorikhalili, S. Cu(OAc)$_2$ Catalyzed Synthesis of Novel Chromeno[4,3-*b*]Pyrano[3,4-*e*]Pyridine-6,8-Dione Derivatives via a One-Pot Multicomponent Reaction in Water under Mild Reaction Conditions. *Polycycl. Aromat. Compd.* **2022**, *42*, 3391–3400. [CrossRef]
75. Pati, S.S.; Singh, L.H.; Guimarães, E.M.; Mantilla, J.; Coaquira, J.A.H.; Oliveira, A.C.; Sharma, V.K.; Garg, V.K. Magnetic chitosan-functionalized Fe_3O_4@Au nanoparticles: Synthesis and characterization. *J. Alloys. Compd.* **2016**, *684*, 68–74. [CrossRef]
76. Bahadorikhalili, S.; Ansari, S.; Hamedifar, H.; Mahdavi, M. The use of magnetic starch as a support for an ionic liquid-β-cyclodextrin based catalyst for the synthesis of imidazothiadiazolamine derivatives. *Int. J. Biol. Macromol.* **2019**, *135*, 453–461. [CrossRef] [PubMed]